



¹⁰Be-based exploration of the timing of deglaciation in two selected areas of southern Norway

Philipp Marr¹, Stefan Winkler², Steven A. Binnie³, and Jörg Löffler¹

¹Department of Geography, University of Bonn, Meckenheimer Allee 166, 53115 Bonn, Germany

²Department of Geography and Geology, University of Würzburg, Am Hubland, 97074 Würzburg, Germany

³Institute for Geology and Mineralogy, University of Cologne, Zùlpicherstr., 49B, 50674 Cologne, Germany

Correspondence: Philipp Marr (marr@uni-bonn.de)

Relevant dates: Received: 18 January 2019 – Revised: 2 May 2019 – Accepted: 13 June 2019 –
Published: 30 July 2019

How to cite: Marr, P., Winkler, S., Binnie, S. A., and Löffler, J.: ¹⁰Be-based exploration of the timing of deglaciation in two selected areas of southern Norway, *E&G Quaternary Sci. J.*, 68, 165–176, <https://doi.org/10.5194/egqsj-68-165-2019>, 2019.

Abstract: We present new ¹⁰Be surface exposure ages from two selected locations in southern Norway. A total of five ¹⁰Be samples allow a first assessment of local deglaciation dynamics of the Scandinavian Ice Sheet at Dalsnibba (1476 m a.s.l.) in southwestern Norway. The bedrock ages from the summit of Dalsnibba range from 13.3 ± 0.6 to 12.7 ± 0.5 ka and probably indicate the onset of deglaciation as a glacially transported boulder age (16.5 ± 0.6 ka) from the same elevation likely shows inheritance. These ages indicate initial deglaciation commencing at the end of the Bølling–Allerød interstadial (~ 14.7 – 12.9 kyr BP) and ice-free conditions at Dalsnibba's summit during the Younger Dryas. Bedrock samples at lower elevations imply vertical ice surface lowering down to 1334 m a.s.l. at 10.3 ± 0.5 ka and a longer overall period of downwasting than previously assumed. Two further ¹⁰Be samples add to the existing chronology at Blåhø (1617 m a.s.l.) in south-central Norway. The ¹⁰Be erratic boulder sample on the summit of Blåhø sample yields 20.9 ± 0.8 ka, whereas a ¹⁰Be age of 46.4 ± 1.7 ka for exposed summit bedrock predates the Late Weichselian Maximum. This anomalously old bedrock age infers inherited cosmogenic nuclide concentrations and suggests low erosive cold-based ice cover during the Last Glacial Maximum. However, due to possible effects of cryoturbation and frost heave processes affecting the erratic boulder age and insufficient numbers of ¹⁰Be samples, the glaciation history on Blåhø cannot conclusively be resolved. Comparing the different timing of deglaciation at both locations in a rather short west–east distance demonstrates the complex dynamics of deglaciation in relation to other areas in southern Norway.

Kurzfassung: Es werden neue ¹⁰Be Oberflächenexpositionsdatierungsalter zweier ausgewählter Lokalitäten in Südnorwegen vorgestellt. Insgesamt fünf ¹⁰Be Altersdatierungen erlauben eine erste Bewertung der lokalen Deglaziationsdynamiken des Skandinavischen Eisschildes auf Dalsnibba (1476 m ü.d.M., über dem Meeresspiegel) im westlichen Südnorwegen. Die Expositionsalter des anstehenden Grundgesteins zwischen 13.3 ± 0.6 und 12.7 ± 0.5 ka vom Gipfel der Dalsnibba indizieren den Beginn der Deglaziation, da das Alter des glazial transportierten Blocks (16.5 ± 0.6 ka) von ähnlicher Höhenlage stammt und dieser wahrscheinlich eine ererbte kosmogene Nuklidkonzentration besitzt. Dies

deutet auf eine beginnende initiale Deglaziation am Ende des Bølling–Allerød interstadial (~ 14.7 – 12.9 kyr BP) und einen eisfreien Gipfel der Dalsnibba während der Jüngerer Dryas hin. Expositionsalter für Grundgestein in niedrigerer Höhenlage weisen auf ein anschließendes Absinken der vertikalen Eisausdehnung auf 1334 m ü.d.M. um 10.3 ± 0.5 ka sowie auf eine länger anhaltende Eisschmelzperiode als bisher angenommen hin. Es werden zwei zusätzliche Datierungen zur bereits bestehenden Deglaziationschronologie von Blåhø (1617 m ü.d.M.) im zentralen Südnorwegen präsentiert. Das ¹⁰Be Alter eines erratischen Blocks auf Blåhø ergibt 20.9 ± 0.8 ka und das erzielte Alter von 46.4 ± 1.7 ka eines Grundgesteinsaufschlusses am Gipfel liegt zeitlich vor dem Spätweichsel-Maximum (LGM). Das ungewöhnlich hohe Grundgesteinssalter lässt sich auf eine ererbte kosmogene Nuklidkonzentration sowie eine Bedeckung mit wenig erosivem, kaltbasalen Eis auf Blåhø während des LGM schließen. Allerdings ist eine abschließende Bewertung der Vergletscherungsgeschichte Blåhø schwierig, da mögliche Effekte von Kryoturbation und Frosthebungsprozessen das Alter des Blocks beeinflussen haben könnten und die Anzahl der Expositionsdatierungen unzureichend ist. Der Vergleich des unterschiedlichen Beginns der Deglaziation in beiden Untersuchungsgebieten in geringer West–Ost Distanz deutet auf komplexe dynamische Deglaziationsprozesse in Relation zu anderen Gebieten in Südnorwegen hin.

1 Introduction

The growth and decay of Quaternary glaciers and ice sheets has had fundamental implications for environmental changes worldwide (Ehlers and Gibbard, 2007). Based on numerical terrestrial or marine radiocarbon and cosmogenic nuclide surface exposure ages in addition to pollen stratigraphy, the chronology of the last deglaciation of the Scandinavian Ice Sheet (SIS) following the Last Glacial Maximum (LGM, 26.5–20 kyr; Clark et al., 2009) and related ice marginal positions in Norway are generally perceived as well constrained (Hughes et al., 2016; Stroeven et al., 2016; Patton et al., 2017). The detailed vertical extent of the SIS in Norway for this period remains, however, uncertain over large areas. Scenarios ranging from maximum models with a central ice dome (Sollid and Reite, 1983; Mangerud, 2004) to minimum models implying a thin multi-domed ice sheet and larger ice-free areas (Dahl et al., 1997; Wohlfarth, 2010) are the topic of ongoing discussion. The knowledge of the vertical dimension of the LGM ice sheet could provide crucial information on palaeoenvironmental factors like sea-level changes, atmospheric and oceanic circulation, (de-)glaciation patterns, ice-sheet erosion rates, landscape evolution, and englacial thermal boundaries (Winguth et al., 2005; Rinterknecht et al., 2006; Goehring et al., 2008). The interpretation of bedrock with different degree of weathering in mountain areas affected by Quaternary glaciation can, therefore, be important for determining ice-sheet behaviour and thickness during the last glaciation periods (Brook et al., 1996; Briner et al., 2006; McCarroll, 2016). There are several concepts to explain the limit between differently weathered bedrock (trimline) separating highly weathered uplands comprising blockfields and tors from relatively unweathered lower exposures of freshly eroded glacial features (Rea et al., 1996; Briner et al., 2006). The two most discussed scenarios suggest on the one hand

the preservation of highly weathered uplands by a cover of non-erosive cold-based ice; thus the trimline would reflect an englacial thermal boundary. The alternative explanation suggests that the trimline represents the true upper vertical ice surface and erosional limit of a former warm-based ice sheet with ice-free nunatak areas above that boundary (Stroeven et al., 2002).

The rise of terrestrial cosmogenic nuclides (TCNs) for surface exposure dating as a key tool to yield numerical ages of landforms and bedrock surfaces representing specific glacier and ice sheet dynamics has revolutionized deglaciation chronologies (Dunai, 2010), especially for settings where organic material is not available for dating. TCNs have been frequently used to reconstruct glacial chronologies worldwide, often utilizing ages derived from erratic boulders or bedrock surfaces (Dunai, 2010; Stroeven et al., 2016, and references therein). To successfully apply TCNs and to establish timing and rates of the last deglaciation, it is necessary that any cosmogenic nuclide produced prior to the last deglaciation has been removed by erosion (Briner et al., 2006; Dunai, 2010). Consequently, the erosive capacity of an ice sheet is mirrored in the concentration of cosmogenic nuclides, as the degree of erosion governs the level of inheritance (Harbor et al., 2006). Erosive capacity is largely causally connected to the basal temperature regime of the ice and its related ability to move by basal sliding. Therefore, cosmogenic nuclide concentrations may also serve as a tool to identify englacial thermal boundaries between warm-based and cold-based zones or estimate palaeo-ice thickness of entirely warm-based glaciers (Kleman, 1994).

The SIS constituted the largest unit of the Eurasian ice sheet (Hughes et al., 2016). Despite the progress with reconstructing volume, margins and timing, the information from terrestrial sources about the former ice cover is limited (Patton et al., 2016). Only a few deglaciation studies have

been carried out in the Geiranger Fjord area in southwestern Norway, where our first selected site, Dalsnibba, is located (e.g. Fareth, 1987; Aarseth et al., 1997). These studies have mostly relied on ¹⁴C dates which have repeatedly been questioned (e.g. Donner, 1996). Hence, only limited numerical age data are available and there is a need for more reliable data for a better understanding of deglaciation dynamics in this area. Our second selected site at Blåhø was previously studied by several authors focussing on deglaciation following the LGM (e.g. Nesje et al., 1994; Goehring et al., 2008; Marr et al., 2018). We provide additional ages from an erratic boulder and from a bedrock outcrop to improve the image of the glaciation history.

In the wake of growing evidence for a more dynamic SIS through the last glacial cycle (Rinterknecht et al., 2006; Mangerud et al., 2010), it is essential to establish a robust deglaciation chronology, particularly for its inner mountainous region, to understand landform evolution and ice sheet dynamics. Given the importance of ice sheets with respect to the climate system, a better understanding of their evolution and the rate and timing of their ice retreat across the mountainous parts of southern Norway is necessary. Here, we report cosmogenic ¹⁰Be surface exposure ages from boulder and bedrock surfaces of two selected mountain sites in southwestern and south-central Norway to improve our knowledge on the (de)glaciation history (Fig. 1). Our main study objectives were as follows:

1. to apply terrestrial cosmogenic ¹⁰Be dating and to determine ¹⁰Be surface exposure ages from the collected boulder and bedrock samples
2. to present the first estimate for the timing of initial local deglaciation for Dalsnibba in Opplendskedalen based on ¹⁰Be
3. to assess and further improve the existing deglaciation chronology for Blåhø in the light of new ¹⁰Be ages presented in this study
4. to explore the ice sheet dynamics and characteristics during the deglaciation in the selected areas in southern Norway.

2 Study area

2.1 Dalsnibba

Dalsnibba (62°4′43 N, 7°17′35 E; 1476 m a.s.l.) is located in Opplendskedalen on the Geirangerfjellet in the western part of south-central Norway. The summit area is dominated by glacially eroded bedrock outcrops which are moderately weathered, but there is no blockfield on Dalsnibba. The general morphology was strongly influenced by Quaternary glaciations with well-developed glacial valleys and deep fjords constituting prevailing macro-landforms (Holstedahl, 1967; Klemsdal and Sjulsen, 1988). Four bedrock samples

from glacially eroded bedrock surfaces and one glacially transported boulder sample taken at four elevations ranging from 1334 to 1476 m a.s.l. were analysed. We aimed for sampling along a vertical transect from Dalsnibba to the valley bottom of Opplendskedalen at ~ 1050 m a.s.l. However, inaccessibility and/or inappropriate sampling sites prohibited us from doing so. Sub-oceanic climatic conditions prevail at the site with mean annual air temperature between 0 and 2 °C (1971–2000) and mean annual precipitation between 2000 and 3000 mm a⁻¹ (1971–2000) (<http://www.senorge.no>, last access: 18 April 2019). The gneiss bedrock is mainly quartz dioritic to granitic and partly migmatitic and is part of the so-called Western Gneiss Region (Tveten et al., 1998). The sampled boulder had the equivalent lithological composition.

The ice retreat following the LGM probably saw the ice margin approaching the inner parts of Storfjorden during the Bølling–Allerød interstadial (~ 14.7–12.9 kyr BP; Patton et al., 2017) when the glacier probably experienced several short standstills in the Geiranger Fjord (Longva et al., 2009). Glaciers readvanced during the Younger Dryas (YD, 12.9–11.7 cal. kyr BP; Lohne et al., 2013) and created moraines at the fjord mouth (Longva et al., 2009). Little is known about the vertical ice limit during the YD; Andersen et al. (1995) suggest a thickness of 800–1200 m in fjords that became ice-free during the Bølling–Allerød interstadial. The final deglaciation following the YD in the fjords in western Norway generally falls between 11.2 ± 0.4 and 10.9 ± 0.2 cal. kyr BP (cf. Nesje and Dahl, 1993; calibration from Hughes et al., 2016, applied).

2.2 Blåhø

Blåhø (61°53′51 N, 9°16′58 E; 1617 m a.s.l.) is located in Otadalen in the central part of southern Norway. Smooth undulating surfaces at summit level are present, with three lower peaks – Rundhø (1556 m a.s.l.), Veslrundhø (1514 m a.s.l.) and Storhøi (1455 m a.s.l.) – part of the mountain ridge. The Blåhø summit is covered by an autochthonous blockfield extending down to a trimline at ~ 1500 m a.s.l. (Nesje et al., 1994). Two samples were collected at the summit: one from a bedrock slab at the eastern edge of the blockfield and one from an erratic boulder. Climatic conditions are continental, with a mean annual temperature of –2 to –1 °C and a mean annual precipitation of 750–1000 mm a⁻¹ at the summit and less than 500 mm a⁻¹ (1971–2000) in the valley (<http://www.senorge.no>); it is among the driest areas in Norway. The area is dominated by quartz-rich Precambrian bedrock. The summit itself is dominated by meta-conglomerate and meta-sandstone on higher and lower slopes, respectively (Tveten et al., 1998). The sampled erratic boulder from the summit is quartz pegmatite.

The (de)glaciation history of Blåhø has attracted researchers' attention for decades (e.g. Nesje et al., 1994; Goehring et al., 2008; Marr and Löffler, 2017). It has been debated whether the summit was covered by cold-based ice

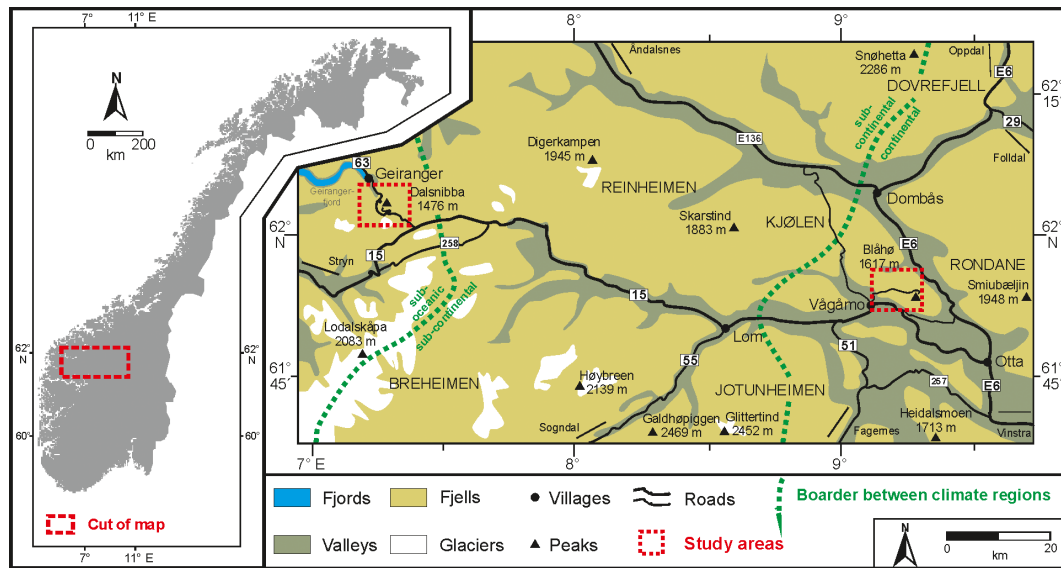


Figure 1. Study areas in southern Norway and the location of Dalsnibba in the west and Blåhø in the east (modified after Löffler and Pape, 2004).

(Goehring et al., 2008) or remained ice-free during the LGM (Nesje et al., 1994). Goehring et al. (2008) established a deglaciation chronology following the LGM, commencing at 25.1 ± 1.8 ka based on a ^{10}Be age from an erratic boulder at the summit to 11.7 ± 1.0 ka at the lowermost sample (1086 m a.s.l.).

3 Methods

3.1 Material and measurement

Surface exposure dating utilizes the in situ build-up of cosmogenic nuclides like ^{10}Be , ^{26}Al or ^{36}Cl by secondary cosmic rays to assess the duration of surface exposure at or near the earth's surface (Balco et al., 2008). The calculation of surface exposure ages using cosmogenic nuclide concentrations from glacial landforms is based on several assumptions. Exposure ages obtained using a single nuclide species are often considered minimum ages, as it is assumed that the samples were constantly exposed at the surface during one single period only, and that they neither contain an inherited nuclide concentration nor were they affected by significant snow shielding or erosion (Stroeven et al., 2002; Briner et al., 2006). In this study, we measured the ^{10}Be concentration of five bedrock (-bed) and two boulder (-bo) samples (Fig. 2). We targeted bedrock outcrops to provide additional new data to existing datasets (Goehring et al., 2008) and to explore the potential thermal and erosional properties of the ice sheet (Harbor et al., 2006; Dunai, 2010) because erratics on top of (glacially modified) bedrock may (Fabel et al., 2002; Dunai, 2010), but not necessarily, provide deglaciation ages (cf. Heymann et al., 2011). It has to be acknowledged, however, that our limited ^{10}Be ages ($n = 7$), especially in the

eastern study area, allow us to improve and assess the existing deglaciation chronology rather than construct an independent one.

The samples were collected by hammer and chisel, and only boulders broader than 20 cm in diameter were selected for measurement to minimize the probability of post-depositional disturbance. All samples were obtained from flat surfaces (dip $< 5^\circ$) with at least 25 cm distance from any edges for the large boulder and the longest distance possible from the edges of the smaller boulder. Both bedrock samples were obtained from locations with weathered surfaces and/or lichen cover to avoid surfaces so intensively weathered that slabs had potentially broken off the boulder surfaces (Fig. S5 in the Supplement). We sampled from local topographic highs to minimize the influence of snow cover. Geographical coordinates and elevations of sampling locations were recorded with a handheld GPS. Topographic shielding was derived from compass and clinometer measurements at each sample site.

After crushing and sieving, between ca. 10 to 44 g of purified quartz was extracted from the rock samples using the approach of Kohl and Nishiizumi (1992). Quartz samples were spiked with around 300 μg of a commercial beryllium solution (Scharlab, 1000 mg L^{-1} , density 1.02 g cm^{-3}) before being dissolved in a concentrated HF/HNO₃ mixture. Preparation of the purified quartz as AMS (accelerator mass spectrometry) targets was undertaken in tandem with a reagent blank. Target preparation chemistry was undertaken in the clean laboratory at the University of Cologne using the single-step column approach described by Binne et al. (2015). Beryllium hydroxide was co-precipitated with Ag, according to Stone et al. (2004), for pressing

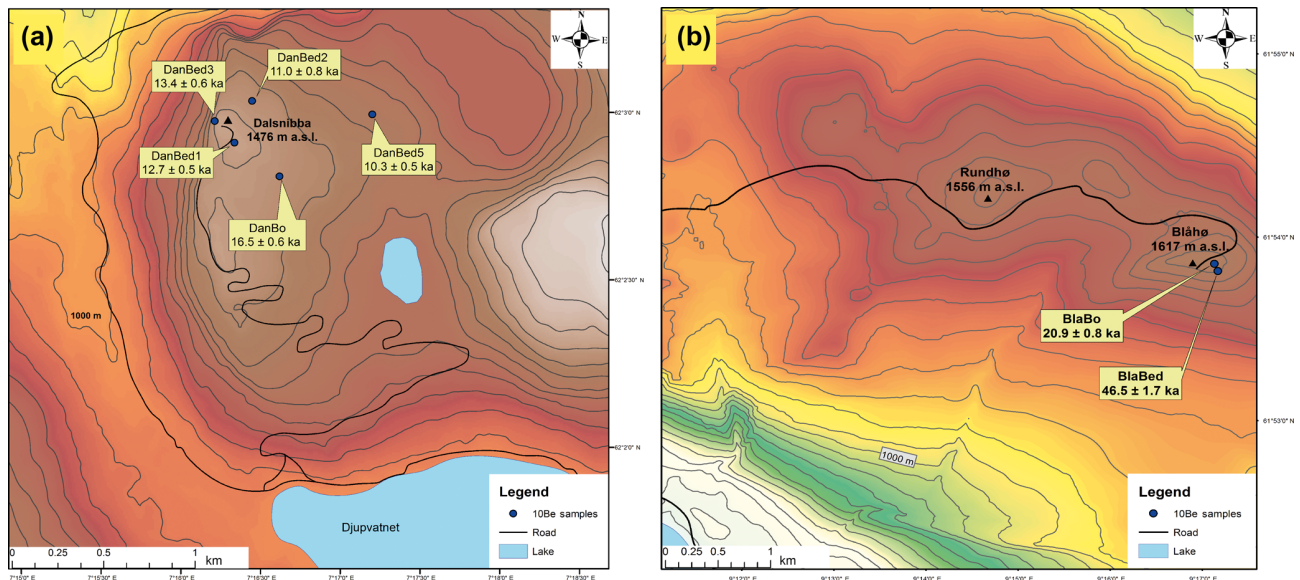


Figure 2. Detailed sampling locations at (a) Dalsnibba and (b) Blåhø. The bedrock samples in both study areas are labelled as -bed, the boulder samples as -bo. The calculated ^{10}Be ages of every sample are reported with 1σ uncertainty in ka. The contour line intervals are a distance of 50 m (source: <http://www.kartverket.no>, last access: 14 January 2019).

into AMS targets. Measurements of $^{10}\text{Be}/^9\text{Be}$ were undertaken at CologneAMS (Dewald et al., 2013), normalized to the revised standard values reported by Nishiizumi et al. (2007). Uncertainties in the blank-corrected ^{10}Be concentrations were derived by propagating (summing in quadrature) the 1 SD uncertainties in the AMS measurements of the blanks and the samples along with an estimated 1 % uncertainty (1 SD) in the mass of ^9Be added as a carrier.

3.2 Exposure age calculations

The ^{10}Be surface exposure ages were calculated with the on-line exposure age calculator version 3, formerly known as the CRONUS-Earth online exposure age calculator (Balco et al., 2008; Balco, 2017; <http://hess.ess.washington.edu/>, last access: 30 April 2019). The spallation-induced regional production rate for western Norway (normalized to sea-level high latitude) was used, as surfaces of unknown age can be dated more precisely due to the proximity of the calibration site (Goehring et al., 2012a, b). We applied the time-dependent LSD scaling model of Lifton et al. (2014) and used the 07KNSTD flag in the online calculator. A rock density of 2.6 g cm^{-3} was applied for all samples. We did not correct our ages for atmospheric pressure anomalies, temporal shielding by snow, sediment or vegetation. Erosion of 1 mm kyr^{-1} was applied in the online calculator, a comparable erosive capacity in summit areas as presented by Andersen et al. (2018a) for Reinheimen, close to Blåhø.

One parameter required within the calibration process for calculating ^{10}Be age is the elevation of the sampled bedrock or boulder surface. Any correction for the effect of post-

glacial glacio-isostatic uplift is, however, quite challenging. No detailed local uplift data for Dalsnibba are available, but an estimate of ca. 100 m total uplift based on reports of former shoreline displacement or modelling attempts seems reasonable (Svendsen and Mangerud, 1987; Fjeldskaar et al., 2000; Steffen and Wu, 2011). For Blåhø, the total postglacial uplift is estimated at around 300 m (Morén and Pässe, 2001). However, this postglacial uplift cannot be described as a linear function as data from other localities in western Norway highlight (e.g. Fjeldskaar, 1994; Helle et al., 2007). An initial strong uplift during Allerød halted during the Younger Dryas and resumed after its termination with high uplift rates in the Early Holocene that subsequently significantly decreased (Lohne et al., 2007). According to newest modelling by Fjeldskaar and Amatonov (2018) the calculated uplift between Allerød and Younger Dryas at around Dalsnibba would summarize to around 50 m, i.e. half of the suggested total postglacial glacio-isostatic uplift. Because postglacial uplift first becomes relevant for ^{10}Be age calculation after exposure of the sampled surface, a circular reference emerges as surface exposure age (the unknown factor itself) needed to be known to precisely determine the amount of uplift that had already occurred according to established models (cf. Jones et al., 2019). To resolve this problem and simplify the correction for postglacial uplift, we assume initial fast uplift between 13 and 11.5 kyr totaling 50 m following Fjeldskaar and Amatonov (2018), followed by linear uplift during the Holocene that accounts for the remaining 50 m. The resulting reduction for sample elevation is ca. 30 m for Dalsnibba. Following similar considerations for Blåhø, a maximum reduction of 150 m in relation to modern elevation is

considered. However, the alternative influence of ca. 100 m reduction and no uplift correction are also assessed because of a likely non-linear uplift function, with maximum uplift during or immediately following deglaciation. The results of different uplift scenarios on Blåhø ages are presented in Table S3 in the Supplement. A reduction of sample elevation of ca. 100 m averaged over the entire surface exposure time seems reasonable and needs to be treated as a maximum value as Early Holocene uplift rates may be underestimated. Finally, with respect to all potential uncertainties with the calculation and calibration of ¹⁰Be surface exposure age estimates (production rates, selected scaling schemes, etc.), our simplified postglacial uplift correction appears appropriate.

4 Results

AMS analysis gave ¹⁰Be/⁹Be ratios ranging from 1.65×10^{-12} to 8.69×10^{-14} . The reagent blank prepared alongside the samples gave a ¹⁰Be/⁹Be value of 6.47×10^{-15} , and the blank subtractions were < 4 % of the total number of ¹⁰Be atoms measured in the samples, aside from sample DanBed2, which yielded less quartz, resulting in a blank subtraction that was 7.5 % of the total.

The cosmogenic exposure ages calculated for all samples from Dalsnibba and Blåhø are shown in Fig. 2 and Table 1. The boulder sample from the summit of Dalsnibba (DanBo) was the oldest from this site at 16.5 ± 0.6 ka. The ¹⁰Be ages from Blåhø are 46.4 ± 1.7 ka (BlaBed) for the bedrock from the blockfield, whereas the boulder resting on the blockfield gave 20.9 ± 0.8 ka (BlaBo). The recalculated ages for Goehring et al. (2008) are presented in Table S4. Results for the effect of different glacio-isostatic uplift rates for Dalsnibba and Blåhø are presented in Tables S2 and S3. The considered uplift of 30 m vs. no uplift for Dalsnibba results in a ~ 3 % age increase. An uplift of 100 m at Blåhø leads to ~ 9 % older ages if compared to no correction for no uplift. For the maximum scenario of 150 m uplift the corresponding value is a ~ 14 % age increase.

5 Discussion

5.1 Methodological considerations and processes affecting ¹⁰Be concentrations

We collected our rock samples from three different settings: bedrock outcrops from weathered debris/blockfields, glacially eroded bedrock surfaces, and boulders. Erosion of the sampled surfaces or undetected shielding (e.g. snow or vegetation cover) would lower the nuclide concentrations and consequently lead to underestimated ages (Stroeven et al., 2002; Hughes et al., 2016). Further, samples collected above the weathering limit, where outcrops are prone to surface degradation by severe frost weathering, also result in an underestimation of the true surface exposure (Brook et al., 1996).

The uplift model used by Goehring et al. (2008) applied on Blåhø reveals ~ 22 % older ages from high-elevation samples (> 1400 m a.s.l.). The recalculated data from Goehring et al. (2008) applying our uplift correction approach (with 100 m) give an estimated age difference of ~ 9 %. A total uplift of 150 m results in ~ 14 % older ages, which is closer to the value obtained by Goehring et al. (2008). For further discussion we rely on the most realistic option with a total uplift of 100 m for Blåhø.

The impact of snow cover on the ¹⁰Be ages was estimated on the basis of Gosse and Philipps (2001) with recent snow conditions (data from <http://www.senorge.no>, averaged 1958–2019). By assuming 150 cm during 9–10 months in the west and 40 cm for 7–8 months (snow density 0.3 g cm^{-3}) in the east are representative of this interglacial, the ¹⁰Be calculations could result in 18 %–20 % too young ages in the west and 4.2 %–4.8 % in the east. It needs, however, to be pointed out that it is impossible to assess whether modern snow conditions are representative of the conditions during the entire Holocene with its known climate variability (Nesje, 2009). We are aware that due to our limited dataset it is impossible to make conclusive statements about the glaciation history, especially for Blåhø, and to definitively identify geological bias and sample outliers (Stroeven et al., 2016). Furthermore, our restrictions to a single cosmogenic nuclide (¹⁰Be) does not allow us to obtain information on any complex burial history that would require pairing ¹⁰Be with other nuclides like ²⁶Al (Fabel et al., 2002). Nevertheless, we assume our results to have the capacity to contribute to the discussion of the timing of deglaciation in both areas because of their generally coherent ages in relation to previously published timings of deglaciation between 11.2 ± 0.4 and 10.9 ± 0.2 cal. kyr BP (cf. Nesje and Dahl, 1993; calibration from Hughes et al., 2016, applied) in the west and 21.8 ± 1.6 ka (Goehring et al., 2008, recalculated) in the east. Recent findings indicate the timing of the last deglaciation at 11 ± 0.2 ka in Reinheimen, located between our study areas (Andersen et al., 2018a).

5.2 Timing of deglaciation at Dalsnibba

The obtained ¹⁰Be surface exposure ages from Dalsnibba offer the possibility of presenting the first age constraints for local deglaciation based on cosmogenic nuclides. The internal consistency of our ¹⁰Be exposure ages from glacially eroded bedrock surfaces with their post-LGM age implies that glacial erosion was sufficient to remove any inherited nuclide concentration, and that the bedrock had been continuously exposed since. This supports the concept that glaciers in fjord landscapes were highly effective erosional agents and consequently warm-based (Aarseth et al., 1997; Matthews et al., 2017), especially in the valleys. This is in agreement with Landvik et al. (2005), who claim that frozen-bed conditions throughout the growth and decay of glaciers in coastal environments are unlikely. However, there are blockfield-covered summits between the fjords which are mostly located at a

Table 1. Sample and laboratory data and calculated ¹⁰Be surface exposure ages.

Sample ID	Sample type	Latitude (°)	Longitude (°)	Altitude (m a.s.l.)	Sample thickness (cm)	Topographic shielding	Blank-corrected ¹⁰ Be conc. (10 ⁵ at g ⁻¹)	Uncertainty (1σ) blank-corrected ¹⁰ Be conc. (10 ³ at g ⁻¹)	External uncertainty (year)	Exposure age (year)
DanBed1	Bedrock	62.047639	7.274044	1476	4.8	0.999935	2.04	8	1100	12700 ± 500
DanBed2	Bedrock	62.049925	7.275275	1418	3.5	0.999997	1.70	13	1200	11000 ± 800
DanBed3	Bedrock	62.049314	7.270258	1464	5.9	0.999976	2.10	8	1200	13300 ± 600
DanBed5	Bedrock	62.048295	7.287856	1334	4.7	0.999544	1.48	6	900	10300 ± 500
DanBo	Boulder	61.897524	9.282407	1438	6.5	1	2.60	10	1500	16500 ± 600
BlaBed	Bedrock	61.897700	9.284238	1615	2.4	1	7.49	26	4200	46400 ± 1700
BlaBo	Boulder	62.044505	7.274839	1617	2.8	1	3.59	14	1900	20900 ± 800

All ages are calculated using version 3 of the calculator code found at <https://hess.ess.washington.edu/> (last access: 30 April 2019) (Balco et al., 2008; Balco, 2017). The western Norway ¹⁰Be production rate (Goehring et al., 2012a, b) is applied with standard atmosphere and pressure “std” and a rock density of 2.6 g cm⁻³. The time-dependent LSD scaling model of Lifton et al. (2014) was used. An uplift for 30 m for Dalsnibba and 100 m for Blåhø was assumed as well as an erosion of 1 mm kyr⁻¹.

higher altitude above the blockfield boundary, indicating that they were potentially protected by cold-based ice (Brook et al., 1996). The two uppermost bedrock ages and the glacial boulder are from comparable altitudinal settings, whereas the boulder is ~ 3.8 to 3.2 ka older than the bedrock samples. This points to inherited cosmogenic nuclide inventory, and we therefore interpret the uppermost bedrock ages ranging from 13.3 ± 0.6 to 12.7 ± 0.5 ka as the timing of deglaciation on Dalsnibba. The bedrock ages mark the subsequent lowering of the ice surface; by plotting sample age with altitude (Fig. S4, $R^2 = 0.91$) the dynamics of ice surface lowering through time becomes clear. As the lowermost sample in this study is at 1334 m a.s.l. (which cannot cover the spectrum until the final downmelt of the ice), the exposure age of the valley bottom of Opplendskedalen (7.47 ± 0.73 ka at 1045 m a.s.l.; Marr et al., 2019) is used to determine the ice surface lowering rate. This gives an ice surface lowering of about 430 m within ~ 5.8 ka. We calculate a thinning rate of ~ 7.3 cm a⁻¹, which is comparable to the inland thinning rate determined by Linge et al. (2007) of 5 cm a⁻¹. We explain this with the persistence of a small ice cap on Dalsnibba and/or glacial readvances (with related fluctuations of the vertical ice limit) as the YD in the valleys probably led to a prolonged ice coverage. Our results from the western study site have three important implications in terms of the local glaciation history:

1. We suggest that the vertical ice limit must have exceeded 1476 m a.s.l. to be able to transport and deposit the boulder at its location. This contrasts to some extent with the view that ice thickness in coastal areas was supposed to be relatively thin due to effective ice drainage (Nesje et al., 1987), but it needs to be considered that Dalsnibba is located at the innermost fjord head of the Geiranger Fjord. Some authors anyway infer the possibility of nunataks on high coastal surfaces in western Norway (Mangerud, 2004; Winguth et al., 2005). In the light of our results, we have to reject the possibility that

Dalsnibba was a nunatak during the LGM but suggest that the summit was covered by warm-based ice.

2. The timing of deglaciation between 13.3 ± 0.6 and 12.7 ± 0.5 ka overlaps with the Bølling–Allerød interstadial, during which the summit of Dalsnibba was probably ice-free, and coincides with when the deglaciation reached Storfjord (Longva et al., 2009). Subsequently, Dalsnibba was not affected by the Younger Dryas readvance. Our results indicate that the deglaciation on Dalsnibba began at the end of the Bølling–Allerød or later, and Dalsnibba constituted a nunatak during the Younger Dryas.
3. There is only sparse information on the final deglaciation in the Scandinavian mountains; it is supposed to have commenced shortly after ~ 10 ka (cf. Hughes et al., 2016). In Reinheimen, east of Dalsnibba, Andersen et al. (2018a) suggest 11 ± 0.2 ka as the timing of the last deglaciation. With our ¹⁰Be results it is difficult to constrain the final deglaciation as our lowermost sample was collected at 1334 m a.s.l. However, we can clearly state that the ice persisted at ~ 1330 m a.s.l. until 10.3 ± 0.5 ka when the final local deglaciation was partly inferred for the region 11.2 ± 0.4 and 10.9 ± 0.2 cal. kyr BP (cf. Nesje and Dahl, 1993; calibration from Hughes et al., 2016, applied). Therefore, our results open up the possibility that the ice coverage at Dalsnibba lasted longer than previously anticipated and also longer than in the Reinheimen area, unless the last part of deglaciation was characterized by a sudden collapse of the remaining ice.

5.3 Implications of ¹⁰Be exposure ages from Blåhø

The ¹⁰Be ages from the blockfield support the overall interpretation that these relict features have survived glaciation with little or no erosion, which indicates long-term landform preservation (Rea et al., 1996; Linge et al., 2006). By acknowledging the widely accepted scenario that anoma-

lously high ^{10}Be concentrations of bedrock samples, such as BlaBed, are the consequence of cold-based ice cover, the blockfield boundary might represent the former englacial boundary between cold-based and warm-based ice (Fabel et al., 2002; Marquette et al., 2004). This implies that the bedrock sample is likely compromised by inherited ^{10}Be from previous exposure followed by preservation beneath cold-based ice (Linge et al., 2006). This scenario appears realistic for the Blåhø bedrock sample, which, consequently, confirms the presence of non-erosive cold-based ice in line with several models suggesting thick ice coverage for this part of Norway (Stroeven et al., 2002; see Goehring et al., 2008). Notably, few of the weighted average bedrock ages from Reinheimen (Andersen et al., 2018a) show inheritance and provide ages of ~ 11 ka. This may point towards different thermal basal ice conditions within a short distance. Cosmogenic ^{10}Be and ^{26}Al nuclide concentration data indicate that some repeatedly glaciated sites have experienced negligible glacial erosion over the entire Quaternary (Briner et al., 2006; Harbor et al., 2006). Therefore, the inherited cosmogenic nuclides must have accumulated during multiple phases of exposure and have subsequently been preserved by cold-based ice (Hughes et al., 2016). Subtracting the exposure age since deglaciation (~ 21 ka) the surface experienced ~ 25 kyr of prior exposure. By using the ice coverage modelled by Mangerud et al. (2010) and Hughes et al. (2016), we evaluate the ^{10}Be concentration accumulation over time (Stroeven et al., 2002). With this approach it seems possible that the bedrock sample on Blåhø was first exposed at the surface during the Early Weichselian or the Eemian interglacial. Some authors suggest even older blockfield ages (e.g. Linge et al., 2006). In this scenario, boulder ages are often considered to reflect the timing of deglaciation (Marquette et al., 2004; Goehring et al., 2008). Following this, our boulder age of 20.9 ± 0.8 ka reflects the beginning of deglaciation, which agrees with the termination of the LGM (Fig. 3). This and the recalculated boulder age of 21.8 ± 1.6 ka (Goehring et al., 2008) supports their statement of the onset of deglaciation around this time. However, alternative interpretations of these boulder ages cannot be rejected, e.g. age overestimation due to post-depositional shielding by burial and subsequent exhumation by frost heave, deposition prior to LGM followed by long-term shielding, or deposition during a readvance following LGM (Briner et al., 2006; Heymann et al., 2011). But Marr et al. (2018) show evidence that the blockfield stabilized ~ 18 ka during severe periglacial conditions, which indicates the absence of ice cover close to the inferred time of boulder deposition.

The alternative interpretation of the bedrock ^{10}Be nuclide concentration assumes continuous surface exposure since at least 46.4 ± 1.7 ka. Geomorphic evidence, such as periglacial activity of the summit blockfield until 18 ka, challenges the inferred presence of cold-based ice on Blåhø during the LGM (Marr et al., 2018). Recently, Andersen et al. (2018b) stated that high-elevation low-relief areas in south-central Norway

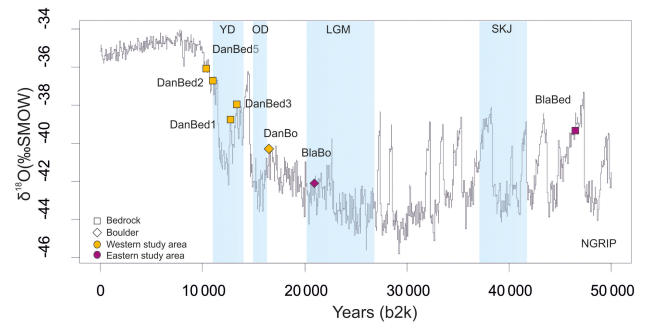


Figure 3. The ages are plotted against the North Greenland Ice Core Project (North Greenland Ice Core Project members, 2004) $\delta^{18}\text{O}$ with ^{10}Be ages. The key cold climate events are the Younger Dryas (YD), Older Dryas (OD), Last Glacial Maximum (LGM) and Skjoghelleren Stadial (SKJ); data are from Clark et al. (2009), Mangerud et al. (2010), Lohne et al. (2013) and Hughes et al. (2016).

were not covered by cold-based but warm-based ice as they calculated significant erosion rates. Therefore, whether the consistent trimline represents an englacial boundary remains ambiguous as englacial thermal boundaries may change frequently and may be unstable over long time periods (Nesje et al., 1987). However, decisive statements on glaciation history based on a single age are not possible; to resolve this issue on Blåhø, more numerical age data are necessary.

5.4 Implications for the regional glaciation history

The time difference of about 6–9 kyr for deglaciation between Dalsnibba and Blåhø is noteworthy. Taking into account the timing of deglaciation at 11 ± 0.2 ka in Reinheimen (Andersen et al., 2018a), located between our study areas, the deglaciation pattern in southern Norway was spatially and temporally variable. In relation to these ages the summit of Blåhø became apparently ice-free relatively early during deglaciation, whereas Dalsnibba at the inner fjord head of Geiranger Fjord became ice-free around 2 kyr later than the Reinheimen plateau. This means that during the YD readvance Reinheimen must have still been ice-covered, but the summit of Dalsnibba was already ice-free.

6 Conclusion

In this paper we present seven in situ cosmogenic ^{10}Be surface exposure ages from two selected mountain locations in southern Norway. Despite uncertainties related to the uncertainties of our ^{10}Be surface exposure ages and the limited dataset, we can delineate age constraints for the timing of deglaciation in the Geirangerfjellet in southwestern Norway. Further, we contribute new age estimates to the previously established deglaciation chronology for Blåhø in south-central Norway. The following conclusions can be drawn from this study:

1. According to the summit bedrock exposure ages ranging from 13.3 ± 0.6 to 12.7 ± 0.5 ka, deglaciation of the summit of Dalsnibba in Opplandskedalen commenced during the termination of the Bølling–Allerød interstadial. The summit successively remained ice-free during the Younger Dryas. However, the ice cover in the valley below the summit lasted longer (until 10.3 ± 0.5 ka) than previously assumed. In contrast to other studies, our results conclude that Dalsnibba was not a nunatak but covered by warm-based ice during the LGM.
2. The bedrock age from Blåhø (46.4 ± 1.7 ka) indicates long-term weathering history and exposure predating the LGM. Most likely, inherited cosmogenic nuclides preserved through shielding by non-erosive cold-based ice are responsible for its old age. However, possible post-depositional disturbance of the boulder and the lack of larger suitable datasets restrict its interpretation.
3. The different timing of deglaciation in both selected sites and in nearby Reinheimen implies complex deglaciation patterns within a spatially limited area. The vertical extent of the Younger Dryas readvance seems to have been less pronounced in the inner fjord areas.

Data availability. All data sources are publicly accessible online; supporting ground imagery can be found in the Supplement.

Supplement. The supplement related to this article is available online at: <https://doi.org/10.5194/egqsj-68-165-2019-supplement>.

Author contributions. PM prepared the manuscript with contributions from all co-authors. SAB was responsible for the ¹⁰Be measurements at CologneAMS.

Competing interests. The authors declare that they have no conflict of interest.

Special issue statement. This article is part of the special issue “Connecting disciplines – Quaternary archives and geomorphological processes in a changing environment”. It is a result of the First Central European Conference on Geomorphology and Quaternary Sciences, Gießen, Germany, 23–27 September 2018.

Acknowledgements. We thank Peter Wilson and one anonymous reviewer for very constructive and thoughtful comments that helped to improve the manuscript. We also thank Tibor Dunai for his expertise and his help. We further acknowledge permission to conduct field work in the Geiranger World Natural Heritage and Landscape Protection Area for over 20 years.

Financial support. This research has been supported by the Friedrich-Ebert-Stiftung (PhD scholarship grant).

References

- Aarseth, I., Austbo, P. K., and Risnes, H.: Seismic stratigraphy of Younger Dryas ice-marginal deposits in western Norwegian fjords, *Norsk Geol. Tidsskr.*, 77, 65–85, 1997.
- Andersen, B. G., Mangerud, J., Sørensen, R., Reite, A., Sveian, H., Thoresen, M., and Bergström, B.: Younger Dryas ice-marginal deposits in Norway, *Quatern. Int.*, 28, 147–169, [https://doi.org/10.1016/1040-6182\(95\)00037-J](https://doi.org/10.1016/1040-6182(95)00037-J), 1995.
- Andersen, J. L., Egholm, D. L., Knudsen, M. F., Linge, H., Jansen, J. D., Goodfellow, B. W., Pedersen, V. K., Tikhomirov, D., Olsen, J., and Fredin, O.: Pleistocene Evolution of a Scandinavian Plateau Landscape, *J. Geophys. Res.-Earth*, 123, 3370–3387, <https://doi.org/10.1029/2018JF004670>, 2018a.
- Andersen, J. L., Egholm, D. L., Knudsen, M. F., Linge, H., Jansen, J. D., Pedersen, V. K., Nielsen, S. B., Tikhomirov, D., Olsen, J., Fabel, D., and Xu, S.: Widespread erosion on high plateaus during recent glaciations in Scandinavia, *Nat. Commun.*, 9, 830, <https://doi.org/10.1038/s41467-018-03280-2>, 2018b.
- Balco, G.: Production rate calculations for cosmic-ray-muon-produced ¹⁰Be and ²⁶Al benchmarked against geological calibration data, *Quat. Geochronol.*, 39, 150–173, <https://doi.org/10.1016/j.quageo.2017.02.001>, 2017.
- Balco, G., Stone, J. O., Lifton, N. A., and Dunai, T. J.: A complete and easily accessible means of calculating surface exposure ages or erosion rates from ¹⁰Be and ²⁶Al measurements, *Quat. Geochronol.*, 3, 174–195, <https://doi.org/10.1016/j.quageo.2007.12.001>, 2008.
- Binnie, S. A., Dunai, T. J., Voronina, E., Goral, T., Heinze, S., and Dewald, A.: Separation of Be and Al for AMS using single-step column chromatography, *Nucl. Instrum. Methods Phys. Res. Sect. B Beam Interact. Mater. Atoms*, 361, 397–401, <https://doi.org/10.1016/j.nimb.2015.03.069>, 2015.
- Briner, J. P., Miller, G. H., Thompson Davis, P., and Finkel, R. C.: Cosmogenic radionuclides from fiord landscapes support differential erosion by overriding ice sheets, *Geol. Soc. Am. B.*, 118, 406–420, <https://doi.org/10.1130/B25716.1>, 2006.
- Brook, E. J., Nesje, A., Lehman, S. J., Raisbeck, R. M., and Yiou, F.: Cosmogenic nuclide exposure ages along a vertical transect in western Norway: Implications for the height of the Fennoscandian ice sheet, *Geology*, 24, 207–210, [https://doi.org/10.1130/0091-7613\(1996\)024<0207:CNEAAA>2.3.CO;2](https://doi.org/10.1130/0091-7613(1996)024<0207:CNEAAA>2.3.CO;2), 1996.
- Clark, P. U., Dyke, A. S., Shakun, J. D., Carlson, A. E., Clark, J., Wohlfarth, B., Mitrovica J. X., Hostetler, S. W., and McCabe, A. M.: The last glacial maximum, *Science*, 325, 710–714, <https://doi.org/10.1126/science.1172873>, 2009.
- Dahl, S. O., Nesje, A., and Øvstedal, J.: Cirque glaciers as morphological evidence for a thin Younger Dryas ice sheet in east-central southern Norway, *Boreas*, 26, 161–180, <https://doi.org/10.1111/j.1502-3885.1997.tb00850.x>, 1997.
- Dewald, A., Heinze, S., Jolie, J., Zilges, A., Dunai, T., Rethemeyer, J., Melles, M., Staubwasser, M., Kuczewski, B., Richter, J., Radtke, U., von Blanckenburg, F., and Klein, M.: CologneAMS, a dedicated center for accelerator mass spectrometry in Germany,

- Nucl. Instrum. Methods Phys. Res. Sect. B Beam Interact. Mater. Atoms, 294, 18–23, <https://doi.org/10.1016/j.nimb.2012.04.030>, 2013.
- Donner, J.: The early and middle Weichselian Interstadials in the central area of the Scandinavian glaciations, *Quaternary Sci. Rev.*, 15, 471–479, [https://doi.org/10.1016/0277-3791\(96\)00002-9](https://doi.org/10.1016/0277-3791(96)00002-9), 1996.
- Dunai, T. J.: *Cosmogenic Nuclides: Principles, Concepts and Applications in the Earth Surface Sciences*, Cambridge University Press, Cambridge, <https://doi.org/10.1017/CBO9780511804519>, 2010.
- Ehlers, J. and Gibbard, P. L.: The extent and chronology of Cenozoic Global Glaciation, *Quatern. Int.*, 164–165, 6–20, <https://doi.org/10.1016/j.quaint.2006.10.008>, 2007.
- Fabel, D., Stroeven, A. P., Harbor, J., Kleman, J., Elmore, D., and Fink, D.: Landscape preservation under Fennoscandian ice sheets determined from in situ produced ¹⁰Be and ²⁶Al, *Earth Planet. Sc. Lett.*, 201, 397–406, [https://doi.org/10.1016/S0012-821X\(02\)00714-8](https://doi.org/10.1016/S0012-821X(02)00714-8), 2002.
- Fareth, O. W.: *Glacial geology of Middle and Inner Nordfjord, western Norway*, Technical Report 408, Geological Survey of Norway, Trondheim, 1987.
- Fjeldskaar, W.: Viscosity and thickness of the asthenosphere detected from the Fennoscandian uplift, *Earth Planet. Sc. Lett.*, 126, 399–410, [https://doi.org/10.1016/0012-821X\(94\)90120-1](https://doi.org/10.1016/0012-821X(94)90120-1), 1994.
- Fjeldskaar, W. and Amatonov, A.: Younger Dryas transgression in western Norway: a modelling approach, *Norsk Geol. Tidsskr.*, 98, 127–139, <https://doi.org/10.17850/njg98-1-08>, 2018.
- Fjeldskaar, W., Lindholm, C., Dehls, J. F., and Fjeldskaar, I.: Post-glacial uplift, neotectonics and seismicity in Fennoscandia, *Quaternary Sci. Rev.*, 19, 1413–1422, [https://doi.org/10.1016/S0277-3791\(00\)00070-6](https://doi.org/10.1016/S0277-3791(00)00070-6), 2000.
- Goehring, B. M., Brook, E. J., Linge, H., Raisbeck, G. M., and Yiou, F.: Beryllium-10 exposure ages of erratic boulders in Southern Norway and implications for the history of the Fennoscandian Ice Sheet, *Quaternary Sci. Rev.*, 27, 320–336, <https://doi.org/10.1016/j.quascirev.2007.11.004>, 2008.
- Goehring, B. M., Lohne, Ø. S., Mangerud, J., Svendsen, J. I., Gyllencreutz, R., Schaefer, J., and Finkel, R.: Late glacial and Holocene ¹⁰Be production rates for western Norway, *J. Quaternary Sci.*, 27, 89–96, <https://doi.org/10.1002/jqs.2548>, 2012a.
- Goehring, B. M., Lohne, Ø. S., Mangerud, J., Svendsen, J. I., Gyllencreutz, R., Schaefer, J., and Finkel, R.: Erratum. Late glacial and Holocene ¹⁰Be production rates for western Norway, *J. Quaternary Sci.*, 27, 544, <https://doi.org/10.1002/jqs.2548>, 2012b.
- Gosse, J. C. and Phillips, F. M.: Terrestrial in situ cosmogenic nuclides: theory and application, *Quaternary Sci. Rev.*, 20, 1475–1560, [https://doi.org/10.1016/S0277-3791\(00\)00171-2](https://doi.org/10.1016/S0277-3791(00)00171-2), 2001.
- Harbor, J., Stroeven, A. P., Fabel, D., Clarhäll, A., Kleman, J., Li, Y., Elmore, D., and Fink, D.: Cosmogenic nuclide evidence for minimal erosion across two subglacial sliding boundaries of the late glacial Fennoscandian ice sheet, *Geomorphology*, 75, 90–99, <https://doi.org/10.1016/j.geomorph.2004.09.036>, 2006.
- Helle, S. K., Rye, N., Stabell, B., Prösch-Danielsen, L., and Hoel, C.: Neotectonic faulting and the Late Weichselian shoreline gradients in SW Norway, *J. Geodyn.*, 44, 96–128, <https://doi.org/10.1016/j.jog.2007.01.001>, 2007.
- Heymann, J., Stroeven, A. P., Harbor, J. M., and Caffee, M. W.: Too young or too old: Evaluating cosmogenic exposure dating based on an analysis of compiled boulder exposure ages, *Earth Planet. Sc. Lett.*, 302, 71–80, <https://doi.org/10.1016/j.epsl.2010.11.040>, 2011.
- Holtedahl, H.: Notes on the formation of fjord and fjord-valleys, *Geogr. Ann. A.*, 49, 188–203, <https://doi.org/10.1080/04353676.1967.11879749>, 1967.
- Hughes, A. L. C., Gyllencreutz, R., Lohne, Ø. S., Mangerud, J., and Svendsen, J. I.: The last Eurasian ice sheets – a chronological database and time-slice reconstruction, *DATED-1, Boreas*, 45, 1–45, <https://doi.org/10.1111/bor.12142>, 2016.
- Jones, R. S., Whitehouse, P. L., Bentley, P. M., Small, S., and Dalton, A. S.: Impact of glacial isostatic adjustment on cosmogenic surface-exposure dating, *Quaternary Sci. Rev.*, 212, 206–212, <https://doi.org/10.1016/j.quascirev.2019.03.012>, 2019.
- Kleman, J.: Preservation of landforms under ice sheets and ice caps, *Geomorphology*, 9, 19–32, [https://doi.org/10.1016/0169-555X\(94\)90028-0](https://doi.org/10.1016/0169-555X(94)90028-0), 1994.
- Klemdal, T. and Sjulsen, E.: The Norwegian macro-landforms: Definition, distribution and system of evolution, *Norsk Geogr. Tidsskr.*, 42, 133–147, <https://doi.org/10.1080/00291958808552192>, 1988.
- Kohl, C. P. and Nishiizumi, K.: Chemical isolation of quartz for measurement of in-situ produced cosmogenic nuclides, *Geochim. Cosmochim. Ac.*, 56, 3583–3587, 1992.
- Landvik, J. Y., Ingólfsson, Ó., Mienert, J., Lehman, S. J., Solheim, A., Elverhøi, A., and Ottesen, D.: Rethinking Late Weichselian ice-sheet dynamics in coastal NW Svalbard, *Boreas*, 34, 7–24, <https://doi.org/10.1111/j.1502-3885.2005.tb01001.x>, 2005.
- Lifton, N., Sato, T., and Dunai, T. J.: Scaling in situ cosmogenic nuclide production rates using analytical approximations to atmospheric cosmic-ray fluxes, *Earth Planet. Sc. Lett.*, 386, 149–160, <https://doi.org/10.1016/j.epsl.2013.10.052>, 2014.
- Linge, H., Brook, E. J., Nesje, A., Raisbeck, G., Yiou, F., and Clark, H.: In situ ¹⁰Be exposure ages from southeastern Norway: implications for the geometry of the Weichselian Scandinavian ice sheet, *Quaternary Sci. Rev.*, 25, 1097–1109, <https://doi.org/10.1016/j.quascirev.2005.10.007>, 2006.
- Linge, H., Olsen, L., Brook, E. J., Darter, J. R., Mickelson, D. M., Raisbeck, G. M., and Yiou, F.: Cosmogenic nuclide surface exposure ages from Nordland, northern Norway: implications for deglaciation in a coast to inland transect, *Norsk Geol. Tidsskr.*, 87, 269–280, 2007.
- Löffler, J. and Pape, R.: Across scale temperature modelling using a simple approach for the characterization of high mountain ecosystem complexity, *Erdkunde*, 58, 331–348, <https://doi.org/10.3112/erdkunde.2004.04.04>, 2004.
- Lohne, Ø. S., Bondevik, S., Mangerud, J., and Svendsen, J. I.: Sea-level fluctuations imply that the Younger Dryas ice-sheet expansion in western Norway commenced during the Allerød, *Quaternary Sci. Rev.*, 26, 2128–2151, <https://doi.org/10.1016/j.quascirev.2007.04.008>, 2007.
- Lohne, Ø. S., Mangerud, J., and Birks, H. H.: Precise ¹⁴C ages of the Vedde and Saksunarvatn ashes and the Younger Dryas boundaries from western Norway and their comparison with the Greenland Ice Core (GICC05) chronology, *J. Quaternary Sci.*, 28, 490–500, <https://doi.org/10.1002/jqs.2640>, 2013.
- Longva, O., Blikra, L. H., and Dehls, J. F.: Rock avalanches: distribution and frequencies in the inner part of Storfjorden, Møre og

- Romsdal County, Norway, Technical Report 2009.002, Geological Survey of Norway, Trondheim, 2009.
- Mangerud, J.: Ice sheets limits in Norway and on the Norwegian continental shelf, in: Quaternary Glaciations Extent and Chronology, edited by: Ehlers, J. and Gibbard, P. L., Elsevier, Amsterdam, 271–294, 2004.
- Mangerud, J., Gulliksen, S., and Larsen, E.: ¹⁴C-dated fluctuations of the western flank of the Scandinavian Ice Sheet 45–25 kyr BP compared with Bølling–Younger Dryas fluctuations and Dansgaard–Oeschger events in Greenland, *Boreas*, 39, 328–342, <https://doi.org/10.1111/j.1502-3885.2009.00127.x>, 2010.
- Marquette, G. C., Gray, J. T., Gosse, J. C., Courchesne, F., Stockli, L., Macpherson, G., and Finkel, R.: Felsenmeer persistence under non-erosive ice in the Tornгат and Kaumajet mountains, Quebec and Labrador, as determined by soil weathering and cosmogenic nuclide exposure dating, *Can. J. Earth Sci.*, 41, 19–38, <https://doi.org/10.1139/e03-072>, 2004.
- Marr, P. and Löffler, J.: Establishing a multi-proxy approach to alpine blockfield evolution in south-central Norway, *AUC Geogr.*, 52, 219–236, <https://doi.org/10.14712/23361980.2017.18>, 2017.
- Marr, P., Winkler, S., and Löffler, J.: Investigations on blockfields and related landforms at Blåhø (Southern Norway) using Schmidt-hammer exposure-age dating: palaeoclimatic and morphodynamic implications, *Geogr. Ann. A.*, 100, 285–306, <https://doi.org/10.1080/04353676.2018.1474350>, 2018.
- Marr, P., Winkler, S., and Löffler, J.: Schmidt-hammer exposure-age dating (SHD) performed on periglacial and related landforms in Opplandskedalen, Geirangerfjellet, Norway: Implications for mid- and late-Holocene climate variability, *Holocene*, 29, 97–109, <https://doi.org/10.1177/0959683618804634>, 2019.
- Matthews, J. A., Shakesby, R. A., and Fabel, D.: Very low inheritance in cosmogenic surface exposure ages of glacial deposits: A field experiment from two Norwegian glacier forelands, *Holocene*, 27, 1406–1414, <https://doi.org/10.1177/0959683616687387>, 2017.
- McCarroll, D.: Trimline trauma: the wider implications of a paradigm shift in recognising and interpreting glacial limits, *Scottish Geogr. J.*, 132, 130–139, <https://doi.org/10.1080/14702541.2016.1157203>, 2016.
- Morén, L. and Pässe, T.: Climate and shoreline in Sweden during Weichsel and the next 150,000 years, SKB Technical Report 01-19, Swedish Nuclear Fuel and Waste Management Co., Stockholm, 67, 2001.
- Nesje, A.: Late Pleistocene and Holocene alpine glacier fluctuation in Scandinavia, *Quaternary Sci. Rev.*, 28, 2119–2136, <https://doi.org/10.1016/j.quascirev.2008.12.016>, 2009.
- Nesje, A. and Dahl, S. O.: Lateglacial and Holocene glacier fluctuations and climatic variations in western Norway: A review, *Quaternary Sci. Rev.*, 12, 255–261, [https://doi.org/10.1016/0277-3791\(93\)90081-V](https://doi.org/10.1016/0277-3791(93)90081-V), 1993.
- Nesje, A., Anda, E., Rye, N., Lien, R., Hole P. A., and Blikra, H.: The vertical extent of the Late Weichselian ice sheet in the Nordfjord-Møre area, western Norway, *Norsk Geol. Tidsskr.*, 67, 125–141, 1987.
- Nesje, A., McCarroll, D., and Dahl, S. O.: Degree of rock surface weathering as an indicator of ice-sheet thickness along an east–west transect across Southern Norway, *J. Quaternary Sci.*, 9, 337–347, <https://doi.org/10.1002/jqs.3390090404>, 1994.
- Nishiizumi, K., Imamura, M., Caffee, M. W., Southon, J. R., Finkel, R. C., and McAninch, J.: Absolute calibration of ¹⁰Be AMS standards, *Nucl. Instrum. Methods Phys. Res. Sect. B Beam Interact. Mater. Atoms*, 258, 403–413, <https://doi.org/10.1016/j.nimb.2007.01.297>, 2007.
- North Greenland Ice Core Project members: High-resolution record of Northern Hemisphere climate extending into the last interglacial period, *Nature*, 431, 147–151, <https://doi.org/10.1038/nature02805>, 2004.
- Patton, H., Hubbard, A., Andreassen, K., Winsborrow, M., and Stroeven, A. P.: The build-up, configuration, and dynamical sensitivity of the Eurasian ice-sheet complex to Late Weichselian climatic and oceanic forcing, *Quaternary Sci. Rev.*, 154, 97–121, <https://doi.org/10.1016/j.quascirev.2016.10.009>, 2016.
- Patton, H., Hubbard, A., Andreassen, K., Auriac, A., Whitehouse, P. L., Stroeven, A. P., Shackleton, C., Winsborrow, M., Heyman, J., and Hall, A. M.: Deglaciation of the Eurasian ice sheet complex, *Quaternary Sci. Rev.*, 169, 148–172, <https://doi.org/10.1016/j.quascirev.2017.05.019>, 2017.
- Rea, B. R., Whalley, W., Rainey, M. M., and Gordon, J. E.: Blockfields, old or new? Evidence and implications from some plateaus in northern Norway, *Geomorphology*, 15, 109–121, [https://doi.org/10.1016/0169-555X\(95\)00118-O](https://doi.org/10.1016/0169-555X(95)00118-O), 1996.
- Rinterknecht, V. R., Clark, P. U., Raisbeck, G. M., Yiou, F., Brook, E. J., Marks, L., Zelčs, V., Lunkka, J.-P., Pavlovskaya, I. E., Piotrowski, J. A., and Raukas, A.: The last deglaciation of the southeastern sector of the Scandinavian Ice Sheet, *Science*, 311, 1449–1452, <https://doi.org/10.1126/science.1120702>, 2006.
- Sollid, J. L. and Reite, J. A.: The last glaciation and deglaciation of Central Norway, in: *Glacial deposits of North-West Europe*, edited by: Ehlers, J., Balkema, Rotterdam, 41–59, 1983.
- Steffen, H. and Wu, P.: Glacial isostatic adjustment in Fennoscandia – A review of data and modeling, *J. Geodyn.*, 52, 169–204, <https://doi.org/10.1016/j.jog.2011.03.002>, 2011.
- Stone, J. O., Fifield, L. K., Beer, J., Vonmoos, M., Obrist, C., Grajcar, M., Kubik, P., Muscheler, R., Finkel, R., and Caffee, M.: Co-precipitated silver metal oxide aggregates for accelerator mass spectrometry of Be-10 and Al-26, *Nucl. Instrum. Meth. B*, 223–224, 272–277, <https://doi.org/10.1016/j.nimb.2004.04.055>, 2004.
- Stroeven, A. P., Fabel, D., Hättestrand, C., and Harbor, J.: A relict landscape in the centre of Fennoscandian glaciation: cosmogenic radionuclide evidence of tors preserved through multiple glacial cycles, *Geomorphology*, 44, 145–154, [https://doi.org/10.1016/S0169-555X\(01\)00150-7](https://doi.org/10.1016/S0169-555X(01)00150-7), 2002.
- Stroeven, A. P., Hättestrand, C., Kleman, J., Heyman, J., Fabel, D., Fredin, O., Goodfellow, B. W., Harbor, J. M., Jansen, J. D., Olsen, L., Caffee, M. W., Fink, D., Lundqvist, J., Rosqvist, G. C., Strömberg, B., and Jansson, K. N.: Deglaciation of Fennoscandia, *Quaternary Sci. Rev.*, 147, 91–121, <https://doi.org/10.1016/j.quascirev.2015.09.016>, 2016.
- Svendsen, J. I. and Mangerud, J.: Late Weichselian and Holocene sea-level history for a cross-section of western Norway, *J. Quaternary Sci.*, 2, 113–132, <https://doi.org/10.1002/jqs.3390020205>, 1987.
- Tveten, E., Lutro, O., and Thorsnes, T.: *Geologisk kart over Norge 1 : 250000, Norges Geologiske Undersøkelse, Ålesund*, 1998.
- Winguth, C., Mickelson, D. M., Larsen, E., Darter, J. R., Moeller, C. A., and Stalsburg, K.: Thickness evolution of the Scandina-

vian Ice Sheet during the Late Weichselian in Nordfjord, western Norway: evidence from ice-flow modeling, *Boreas*, 34, 176–185, <https://doi.org/10.1111/j.1502-3885.2005.tb01013.x>, 2005.

Wohlfarth, B.: Ice-free conditions in Sweden during Marine Oxygen Isotope Stage 3?, *Boreas*, 39, 377–398, <https://doi.org/10.1111/j.1502-3885.2009.00137.x>, 2010.